

Photogrammetric Approach to Aerial Thermal Survey

Dr. Qassim Abdullah Raven McDavid Brandon McKenzie Darin David

Woolpert, Inc.

4454 Idea Center Boulevard

Dayton, OH 45430-1500

Abstract

Today's emphases on energy conservation are at their highest peak, as federal regulations require public facility managers to meet certain standards of energy efficiency. Aerial thermal survey can play a key role in providing these managers with an efficient and robust means to derive information that helps them in collecting metrics on energy use and energy auditing. For these managers to rely on the products from aerial thermal surveys, they need them to fit seamlessly into their existing Geographic Information System (GIS) database. Unfortunately, aerial thermal surveys in most cases were conducted in a haphazard fashion, lacking the quality and the high geometrical fidelity that characterize the different GIS layers. This paper introduces an end-to-end photogrammetric approach for acquiring and processing aerial thermal data including the extraction of digital surface model (DSM) from thermal imagery. Besides detailing best practices necessary for the photogrammetric thermal data work flow, the paper discusses in detail the work flow and the positional accuracy achieved from state-of-the-art thermal sensors. The paper also discusses results from different processing software.

Introduction

As early as 1974, the U.S. Army Facility for Engineer Support Agency (FESA) and the U.S. Army Cold Region Research and Engineering Laboratory (CRREL) began investigating Infrared Thermography (IT) as a means for evaluating and detecting the presence of entrapped moisture in roofing systems. The methods were later adopted by the U.S. Air Force; a number of agencies within the government for their research, such as the National Institute for Standards and Technologies (NIST) (formerly the National Bureau of Standards); NASA; University of Michigan; and South Dakota State University (Tobiasson, 1982) (Tobiasson and Korhonen, 1978), (Sopko, 1981). Because of the common use of large buildings with flat roofs within the defense and other federal establishments, early applications of IT heavily focused on building roof inspection (Abdullah and Kreighbaum, 1999) (Abdullah and McClellan, 2011). The use of IT grew with time to include the inspection of buried hot water and steam pipes, which was encouraged by the fact that IT provides a nondestructive inspection tool. Engineers and facility managers are always challenged by the decision to dig a network of hot water or steam pipes established under busy roads to inspect and locate a poor-performing segment of the network. The principal author of this paper was involved in designing and executing two thermal surveys to inspect the underground steam conduits at the Naval Academy and the city of Manhattan, NY. The latter survey was used to estimate the increasing amounts of energy loss from the complex system of steam conduits buried under the city of Manhattan. Aerial IT succeeded in gathering evidence and pinpointed the locations within the steam pipes network under Manhattan that were in most urgent need for repair.

The recent focus on sustainability and energy conservation and audits opened new and strong demands for this nondestructive inspection method of IT. On October 5, 2009, the president of the U.S. issued an executive order entitled “Federal Leadership in Environmental, Energy, and Economic Performance.” Article g of the executive order calls for the implementation of high performing sustainable federal building design, construction, operation and management, maintenance, and deconstruction as stated in the following selected clauses of the article:

- i. Beginning in 2020 and thereafter, ensuring that all new Federal buildings that enter the planning process are designed to achieve zero-net-energy by 2030;*
- iii. Ensuring that at least 15 percent of the agency's existing buildings (above 5,000 gross square feet) and building leases (above 5,000 gross square feet) meet the Guiding Principles by fiscal year 2015 and that the agency makes annual progress toward 100-percent conformance with the Guiding Principles for its building inventory;*
- v. Managing existing building systems to reduce the consumption of energy, water, and materials, and identifying alternatives to renovation that reduce existing assets’ deferred maintenance costs.*

All these potential applications of IT opened business opportunities for many. Among such opportunities is the aerial IT survey of facilities and campuses. The aerial survey includes the acquisition of hundreds, if not thousands, of aerial thermal images that need to be co-located spatially to form a seamless mosaic that can be added as a layer to existing GIS utilized by facilities managers and engineers. Unfortunately, most aerial IT providers in the past followed a non-geospatial approach as their data in most cases could not accurately be utilized as a layer in an existing GIS for the lack of accurate geo-referencing. Part of the reason that their data lacked the geometrical accuracy was due to the challenging nature of the thermal signature of ground objects and the non-metric sensors used for such surveys. In the following sections, a complete photogrammetric workflow will be described that enables the researchers to obtain high geospatial accuracy that meets map accuracy standards.

Study Area

Two areas were chosen for the analysis. Those are:

The University of Dayton Campus: The campus is located in the city of Dayton, Ohio and covers an area of approximately 1.7 square kilometers of mixed land cover and mixed land use.

The Wright State University Campus: The campus is also located near the city of Dayton, Ohio and covers an area of approximately 2.5 square kilometer of mixed land cover and mixed land use.

The two sites were flown with slightly different parameters. This will be detailed in the following sections.

Project Design

The two sites were flown according to the following flying parameters:

Site	Flying Altitude AGL (meter)	Resulting GSD (meter)
University of Dayton Campus	880.0	0.25
The Wright State University	800.0	0.22

Materials and Methods

Thermal Sensor:

The researchers used a high-end thermal sensor from FLIR Systems, Inc. The sensor, model SC8303, of Figure 1 has high-speed MWIR science-grade infrared cameras with high resolution and highly sensitive cooled detectors. Such a sensor is usually used for studies that require the most accurate thermal measurements and recordings. Besides its high sensitivity, the SC8303 is considered one of the highest resolution sensors available in the market today with an array size of $1,344 \times 784$ pixels. Table 1 lists various characteristics for the SC8303. A lens with focal length of 50 mm was utilized with the sensor to acquire the thermal imagery.

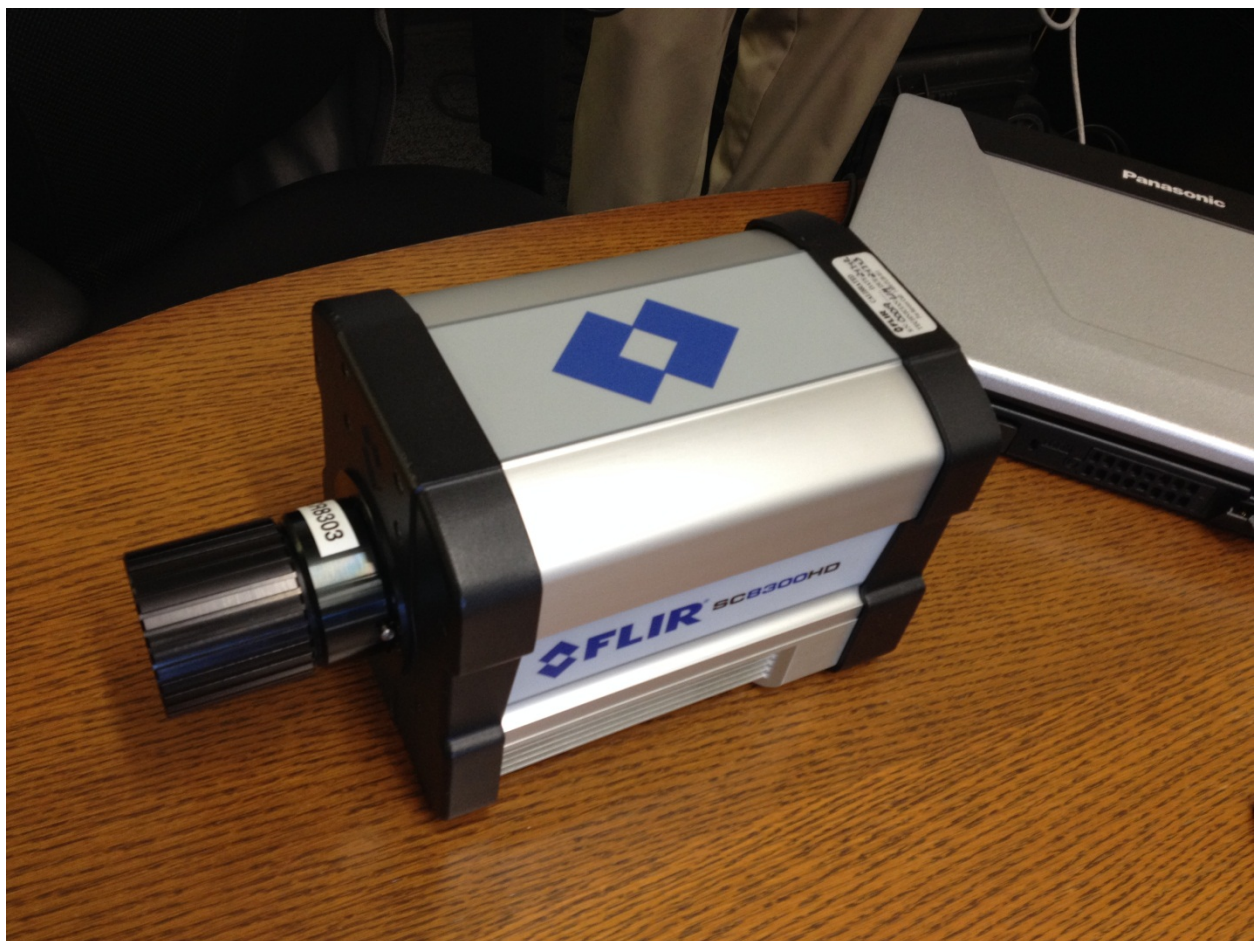


Figure 1 FLIR SC8303 thermal camera (courtesy: FLIR Systems, Inc.)

Table 1 Technical specification for FLIR SC8303

Detector Type	Indium Antimonide (InSb)
Spectral Range	1.5 – 5.0 μm
Resolution	1,344 \times 784
Detector Pitch	14 μm
Noise Equivalent Temperature Difference (NETD)	0.0068° C (<25 mK)
Well Capacity	5.9 M electrons
Frame Rate (Full Window)	132 Hz
Dynamic Range	14-bit
Standard Temperature Range	-20°C to 500°C (-4°F to 932°F)
Accuracy	\pm 2°C or \pm 2% of Reading
Sensor Cooling	Closed Cycle Linear

Ground Control Network:

Due to the challenging nature of the thermal signature of ground feature, the researcher came to the realization that deriving ground control points from an existing geometrically accurate orthoimagery and high definition accurate digital terrain model is the best and safest approach for the study. Existing high-resolution imagery provides flexibility in selecting as many ground control locatons as needed throughout the study area. For this purpose, orthoimagery from the Ohio Statewide Imagery Program (OSIP) with a ground resolution of 15 cm were used.

Second Generation Control Extraction

To establish ground control, well defined photo ID control points were observed both in the thermal imagery and in an existing OSIP 15 cm natural color ortho dataset for each area of interest (AOI). Using a COTS data viewer (Global Mapper), XY coordinates were extracted from the color orthoimagery, while Z values were extracted from an existing dense Lidar dataset.

Despite the fact that the thermal imagery was dark with low contrast, the actual semi-automatic pixel matching worked well. Warm and hot features including light poles, catch basins, manhole lids, pavement edges and sidewalks appeared clearly in the thermal imagery and created good photo identifiable targets in the orthoimagery.

These second-generation XYZ values were used as ground control in the absolute orientation, producing refined exterior orientation values to use in the ortho-rectification of the thermal imagery.

Data Processing

The processing followed a traditional photogrammetric workflow starting with aerial triangulation and ending with ortho-rectification and mosaicking of the data. Since they represent a record for the level of heat emitted from ground objects, thermal imagery lacks the visual distinction of ground features that we are accustomed to in standard imagery. The researchers investigated three different commercial

photogrammetric processing software packages to determine the most efficient software that can work reliably with thermal imagery. One of the software programs is a well-known conventional photogrammetric program, while the other two utilize some computer vision techniques to augment the photogrammetric modeling.

Photogrammetric versus computer vision techniques

In an aerial image-based mapping, the process of aerial triangulation (AT) is performed to expand or densify the ground control network within a block of captured imagery for improved photogrammetric measurement in subsequent applications. Prior to the expansion of ground control through the AT process, suitable methods for identifying and measuring image pass and tie points from an aerial thermal Infrared (TIR) imagery survey were tested. The University of Dayton and Wright State University project areas are far too large to rationalize manual measurement of image pass and tie points. Such work requires a semi-automated AT approach, one that systematically parses image redundancy, efficiently identifies key features, accurately measures and matches such features in thermal IR imagery, and will generate sufficient pass and tie points for the AT process.

Several conventional photogrammetric software programs offer automated tie point extraction modules that apply normalized cross-correlation image matching either by area-based, feature-based, or Semi-Global Matching (SGM) methods. Such image matching runs numerical comparisons of image digital numbers by pixel sub-array or at the pixel level computing linear regression analysis, or by an iterative least squares best fit for deriving acceptable matches. Feature-based matching provides an alternative to searching all image locations by extracting feature regions, but the cross correlation of feature regions are detected on non-affine invariant approaches and thus more susceptible to image noise and scale variance (Lowe 1999). Dense matching of SGM are supported by global cost functions not oriented along image scan line, but optimized symmetrically in eight path directions towards all pixels within the image for efficient pixel level approximations (Hirschmuller 2008). Normalized cross-correlation methods can be highly dependent on accurate camera modeling and initial image orientation, and consequently will have difficulty converging into adequate solution under sizeable variations in illumination, scale, rotation, and 3D projection (Paul R. Wolf, Bon A. Dewitt et al. 2014). This research tests the capacity of conventional photogrammetric software to accurately match pass and tie points in thermal IR imagery during the AT process in the absence of and a working camera model, gyro stabilized camera mount, and no initial image orientation measurements.

New photogrammetric software now incorporates Computer Vision (CV) techniques in automated tie point extraction capable of robust image matching more tolerable of variations in image intensity, scale, rotation, lens distortion, and changes in affine projection. Some CV approaches work to transform an image into a collection of local feature vectors sampled at numerous repeatable image locations, each invariant to image scaling, translation, rotation, and partially invariant to image intensity and variations in 3D projection (Lowe 1999). The computational cost of extracting such features is minimized by applying a cascading filter of difference-of-Gaussian function image pyramids, focusing expensive computations toward identifying key points invariant of scale, and transforming distinctive descriptors and gradient orientations which pass certain stability and Euclidean distance criteria (Lowe 2004). More recently, some CV approaches are optimized for higher resolution imagery and very dense point matching by aggregating layers from the cascading approach of Gaussian filters into orientation histograms, or depth maps by pixel which maintain the same invariance but can be computed even more efficiently yielding very dense point spacing (Tola, Strecha et al. 2012). In the photogrammetric CV approach, image matching invariant of image intensity, scale, and rotation are the basis for which very dense point matches are refined using the collinearity equations and least squares bundle adjustments

of the AT process. This eliminates the requirements for working camera model, camera stabilization, and accurate initial image orientation measurements as prerequisites for the AT process. This research also tests the effectiveness of photogrammetric CV software to accurately match pass and tie points in thermal IR imagery during the AT process given the unknown parameters previously described.

Processing Method I (Conventional Solution)

The auto-correlation of tie and pass points was challenged by the fact that the thermal imagery did not have the fine details of standard imagery, to which this software is accustomed. In addition, two operational incidents occurred during the aerial data acquisition that may have contributed to the less than optimum performance of this software. Those incidents are:

The Failure in Recording Airborne GPS: Due to a technical reason, none of the airborne GPS data recorded during the flight was usable to support GPS-based aerial triangulation.

The Absence of Geometrical Camera Calibration Report: The SC8303 was never calibrated and only an estimate for some of the interior geometry parameters, namely focal length and CCD size, are available. There was no information available about the location of the principal point. Moreover, the operator needed to adjust the focusing ring during flight in to remove the blurring he noticed in the imagery if he sets the lens focus to infinity. Such refocusing altered the value of the focal length by an unknown value which made it even more challenging for the processing software.

The Absence Gyro-stabilized Mount: The camera was not mounted on a stabilization mount as it was fitted in the aircraft. This caused large variation in camera rotation angles. The final adjusted Omega angle values ranged from 13.8 to -11.9 degrees. The final adjusted Phi angle values ranged from 6.7 to -4.3 degrees. This caused wide variations in side lap.

Considering all of the above-listed challenges, the software failed to generate a well-distributed dense network of tie and pass points and failed to perform a reliable camera self-calibration despite the fact that enough second-generation ground control points were provided during the aerial triangulation solution. A conventional aerial triangulation solution was reasonably achieved and camera exterior orientation parameters for all the frames were determined to a satisfactory accuracy for both study areas.

Processing Method II (Hybrid Solution)

The software used here is originally a conventional photogrammetric package that was modified to deal with imagery from an Unmanned Aerial System (UAS). It is understood that some of the CV techniques were added at some stages of the processing. Due to time constraints, only thermal imagery from the University of Dayton campus was processed using this method. The software failed to process the data without providing it with approximate camera position for all the frames. The exterior orientation parameters produced from Processing Method I were provided to the software. Afterwards, the software was able to auto-correlate a decent amount of tie and pass points and perform camera self-calibration through which the correct value for the focal length was computed.

Processing Method III (Hybrid Solution)

The software used here is largely associated with processing imagery from a UAS, and it relies on CV techniques for the majority of its operations. Due to time constraints, only thermal imagery from the University of Dayton campus was processed using this method. Similar to the software used in

Processing Method II, once the exterior orientation parameters generated by Processing Method I were provided to the software, the software was able to generate a dense network of tie and pass points and perform camera self-calibration. A small number of ground control points were utilized in the solution that resulted in acceptable results. This software was unique in the sense it was able to generate an auto-correlated digital surface model that was used for the ortho-rectification process of the imagery. None of the other two software packages were able to produce a digital surface model. Figure 2 shows the digital surface model generated from the thermal imagery for the University of Dayton campus.

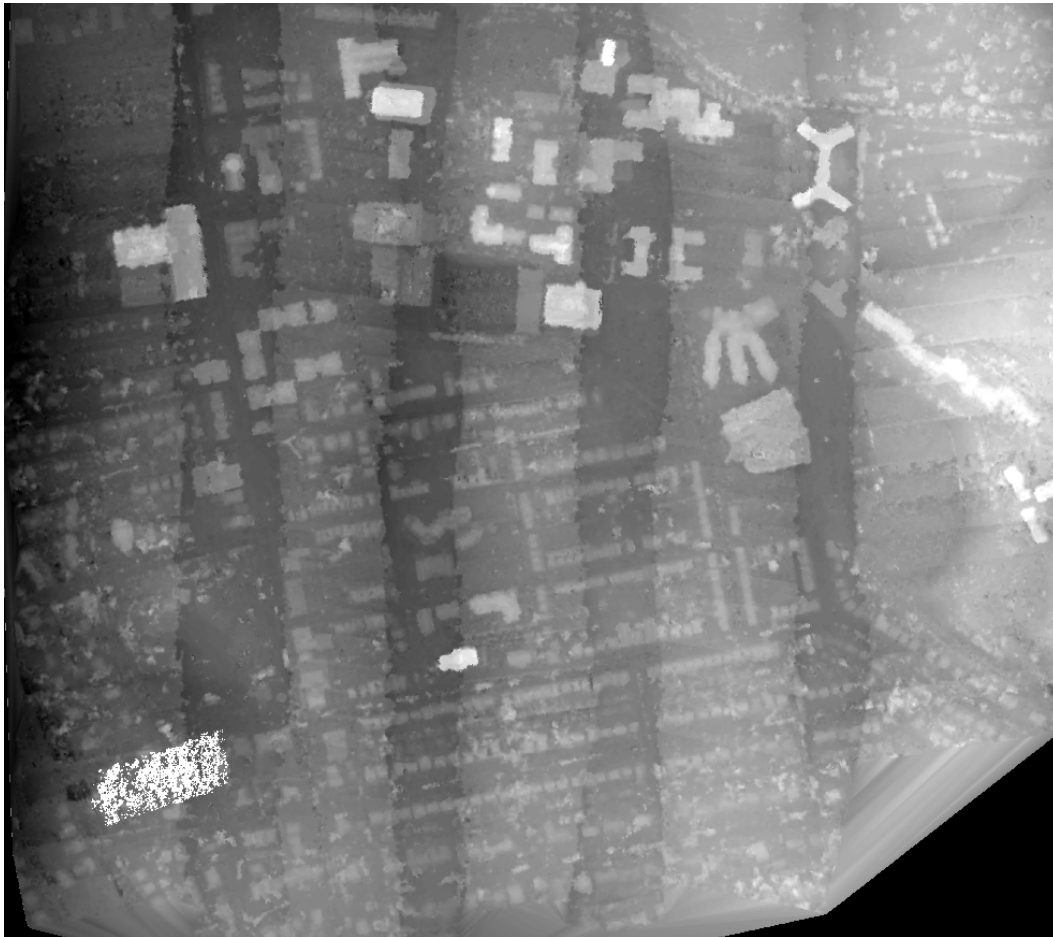


Figure 2 Digital surface model generated from the thermal imagery for the University of Dayton campus (courtesy: Woolpert, Inc.)

Ortho-rectification of Thermal Imagery

The finalized aerial triangulation (absolute orientation) solution from Method I was used together with the thermal imagery and the Lidar dataset to ortho rectify the thermal imagery. As for Method II and III, after measuring the ground control points, the process was run in an automated mode without operator intervention to produce the final orthoimagery. Orthoimagery with a ground sample distance (GSD) of 30 cm were generated for both study areas from all three methods.

Mosaicking

In Method I, the rectified thermal imagery was then processed using the mosaicking software to create a seamless mosaic image. Figure 3 shows the extents of the frames used in Method I to generate the thermal mosaic for the University of Dayton campus. Again for Methods II and III, the processing of mosaic was performed in the back ground without user intervention.

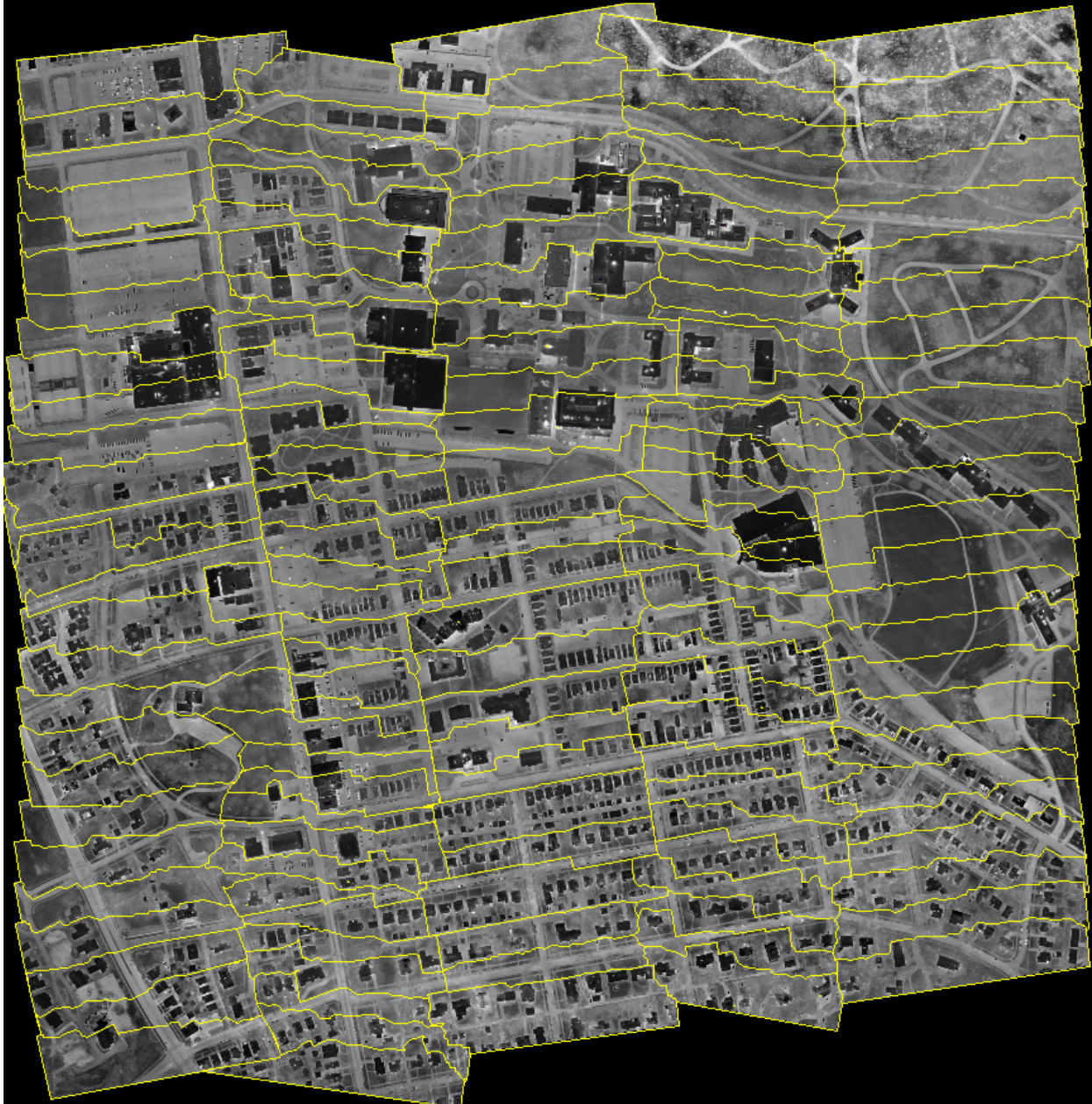


Figure 3 Thermal mosaic of the University of Dayton campus (courtesy: Woolpert, Inc.)

Accuracy Assessment

To determine the accuracy of the generated thermal mosaics, another set of photo-identifiable ground checkpoints was extracted for each study area using the OSIP orthoimagery. After rectification, the accuracy of the thermal mosaic for the University of Dayton produced from each of the three methods was evaluated using the extracted set of photo-identifiable check points. Table 2 shows the results of such evaluation. The only mosaic for the Wright State University campus produced using Method I was also evaluated in a similar fashion. Table 3 shows the results of evaluating the mosaic from Method I for Wright State University campus.

Table 2 Accuracy evaluation from the three methods for the University of Dayton campus

Point ID	Method I		Method II		Method III	
	ΔE (Easting)	ΔN (Northing)	ΔE (Easting)	ΔN (Northing)	ΔE (Easting)	ΔN (Northing)
	(meter)	(meter)	(meter)	(meter)	(meter)	(meter)
0	-0.258	-0.012	0.201	-0.446	0.012	-0.409
1	-0.363	0.218	0.090	-0.224	-0.391	0.127
2	0.250	-0.097	0.409	-1.010	-0.343	0.827
3	0.226	-0.667	-0.074	-0.374	-0.600	0.108
4	0.369	-0.062	0.393	-0.257	-0.095	1.005
5	0.028	0.596	-0.379	-0.372	-0.831	-0.041
6	-0.086	0.278	0.588	0.408	0.682	0.164
7	-0.294	0.550	0.032	-0.849	-0.118	0.132
8	0.048	0.838	0.362	-0.499	-0.424	-0.444
9	0.131	0.257	-0.122	-0.178	-0.141	0.324
10	0.381	-0.196	-0.099	0.401	0.205	0.447
11	0.021	-0.203	0.153	-0.277	0.571	-0.500
12	-0.079	0.232	0.830	-0.351	0.347	-0.651
13	0.215	0.292	0.155	-0.354	-0.014	-0.584
14	-0.125	-0.380	0.499	-0.248	0.627	0.077
15	-0.207	0.108	-0.056	-0.380	0.071	-0.241
16	-0.677	0.114	0.655	-0.441	0.464	-0.069
17	-0.100	-0.321	0.238	-0.527	0.083	-0.519
18	-0.067	-0.686	0.171	-0.526	-0.069	0.473
19	0.026	0.202	-0.013	-0.304	-0.511	0.090
20	0.180	0.396	-0.266	-0.155	0.151	0.199
21	-0.276	0.209	0.561	-0.185	1.081	-0.424
22	-0.820	-0.091	-0.137	-0.608	0.260	0.641
23	-0.729	-0.331	0.012	-0.255	0.192	0.162
24	-0.820	-0.058	0.218	-0.658	0.005	0.321
25	-0.347	0.171	0.116	-0.544	0.663	0.425
26	0.297	-0.074	0.083	-0.022	-0.127	0.268
27	-0.080	-0.423	-0.391	-0.217	-0.382	-0.076
28	0.593	0.233	-0.430	0.107	-0.673	-0.067
29	0.032	0.476	0.387	-0.091	0.383	0.101

Mean	-0.084	0.052	0.140	-0.315	0.036	0.062
StDEV	0.354	0.359	0.316	0.302	0.449	0.413
RMSE	0.358	0.357	0.341	0.432	0.443	0.410
95% Accuracy	0.875 meter		0.953 meter		1.045 meter	

Table 3 Accuracy evaluation from method I for the Wright State University campus

Point ID	Method I	
	ΔE (Easting)	ΔN (Northing)
	(meter)	(meter)
0	-0.313	0.716
1	-0.159	0.897
2	-0.053	0.511
3	-0.530	0.198
4	-0.152	0.730
5	-0.438	0.506
6	-0.036	0.274
7	-0.344	0.194
8	-0.284	-0.185
9	-0.131	-0.292
10	-0.604	0.110
11	0.888	0.458
12	0.860	0.849
13	0.289	0.102
14	-0.626	-0.257
15	0.326	-0.376
16	0.152	-0.218
17	-0.067	-0.196
18	-0.612	-0.172
19	-0.993	-0.709
20	-1.085	-0.629
21	0.055	-0.152
22	-0.168	-0.220
23	-0.231	-0.638
24	-0.061	-0.739
25	-0.788	0.034
26	-0.280	-0.476
27	-0.160	-0.261
Mean	-0.198	0.002
StDEV	0.455	0.477
RMSE	0.489	0.468

95% Accuracy	1.171 meter
-------------------------	--------------------

Results Analysis:

The final accuracy results of the thermal orthoimagery from the three methods were within 15 cm (half pixel) from one method to another and within 40 cm (about 1.5 pixel) from the OSIP orthoimagery. With the absence of ground surveyed ground control, it is difficult to state the exact absolute accuracy of the thermal orthoimagery. All that can be done in this case is to compare it to the accuracy of the OSIP orthoimagery. The OSIP orthoimagery with 15 cm GSD were produced to meet an accuracy of 30 cm RMSE. Actual accuracy for the OSIP orthoimagery as delivered by vendors is expected to be better than 30 cm; however, for the sake of evaluating the thermal orthoimagery, it will be assumed that the OSIP orthoimagery are only accurate to 30 cm RMSE. Since the thermal orthoimagery are accurate to about 40 cm in reference to the OSIP orthoimagery, one can easily conclude that the absolute accuracy of the thermal orthoimagery is expected to be around 60 cm RMSE, or two ortho pixels.

Conclusions and Recommendations

The study resulted in the following conclusions:

1. Data from aerial thermal survey can be added to an existing accurate GIS database by following photogrammetric approach.
2. Recently introduced processing software packages that were designed to serve the UAS community can easily be adapted to process thermal imagery. Such software can result in a highly productive workflow.
3. Carefully planned and executed thermal surveys can result in thermal orthoimagery with accuracy that matches the accuracy of standard orthoimagery with the same ground resolution.
4. It is possible to produce auto-correlated digital surface model from thermal imagery that can be used to accurately ortho-rectify the thermal imagery.
5. It is possible to perform accurate in-situ camera calibration using software mentioned in point 2 above.

It is recommended to consider the following items:

1. **The importance of producing accurate time events during the camera firing of each frame:**
Such time events can be used to interpolate camera positions that are needed for the processing software.
2. **Laboratory calibration of the thermal camera to determine its interior orientation parameters:**
This can add to the accuracy of the products and may result in more efficient processing workflow.
3. **Mounting the thermal camera on a stabilization mount:**
This is highly recommended to reduce the large amount of side lap that is otherwise needed to prevent coverage gaps.
4. **Second generation controls concept (from existing orthoimagery):**
This provides flexibility in the workflow and reduces costs as long as the final accuracy of the products is considered in the project design.

Acknowledgments

The authors would like to acknowledge the assistance they received from Dan Michalec, Brian Albers, Joe Cantz, Layton Hobbs and Bob Shelton. All are with Woolpert, Inc.

References

- Abdullah, Q. and D.W. Kreighbaum, 1999. "Airborne infrared thermography for detection of moisture damage on built-up roofs", Proceedings of the ASPRS annual convention, Portland, Oregon
- Abdullah, Q. and R. McClellan, 2011. "Airborne infrared thermography for environmental and facility management of the army National Guard training facilities" Proceedings of the ASPRS Fall convention, Herndon, Virginia.
- Hirschmuller, H. (2008). "Stereo processing by semiglobal matching and mutual information." Pattern Analysis and Machine Intelligence, IEEE Transactions on 30(2): 328-341.
- Lowe, D. G. (1999). "Object recognition from local scale-invariant features", Computer vision, 1999. The proceedings of the seventh IEEE international conference on, Ieee.
- Lowe, D. G. (2004). "Distinctive image features from scale-invariant keypoints", International journal of computer vision 60(2): 91-110.
- Sopko, V. (1981). "Detection of moisture in commercial and industrial built-up roofing systems", Proceedings, Thermosense IV, Society of Photo-Optical Engineers. v. 313, pp. 114-118.
- Tobiason, W. (1982). "Roof moisture surveys: current state of the technology", Proceedings, Thermosense V, Society of Photo-Optical Engineers. v. 371, pp. 24-30.
- Tobiasson, W., and Korhonen, C. (1978). "Summary of Corps of Engineers Research on Roof Moisture Detection and Thermal Resistance of Wet Insulation", U.S. Army Cold Regions Research and Engineering Laboratory Special Report 78-29.
- Tola, E., C. Strecha, et al. (2012). "Efficient large-scale multi-view stereo for ultra high-resolution image sets" Machine Vision and Applications 23(5): 903-920.
- Wolf, P., Bon A. Dewitt, et al. (2014). "Elements of Photogrammetry with Applications in GIS", Fourth Edition, McGraw Hill Professional, Access Engineering.